

Phosphate removal using novel combined Fe-Mn-Si oxide adsorbent

Fe-Mn-Si 산화물을 이용한 인 제거 흡착 연구

Minsoo Maeng · Haegyun Lee · Seok Dockko*

맹민수 · 이해균 · 독고석*

Dept. of Civil and Environ. Eng., Dankook Univ.

Abstract : The removal of phosphate from surface water is becoming increasingly vital to prevent problems such as eutrophication, particularly near urban areas. Recent requirements to reduce high concentrations of phosphate rely on physicochemical methods and adsorbents that must be effective even under strict conditions. The phosphate removal efficiencies of two adsorbents, Fe-Mn-Si oxide and Fe-Mn oxide, were investigated and the data used to compare kinetics and isotherm models. The maximum adsorption capacities of the two adsorbents were 47.8 and 35.5 mg-PO₄³⁻/g, respectively. Adsorptions in both cases were highly pH dependent; i.e., when the pH increased from 3 to 9, the average adsorption capacities of the two adsorbents decreased approximately 32.7 % and 20.3 %, respectively. The Freundlich isotherm model fitted the adsorption of Fe-Mn-Si oxide more closely than did the Langmuir model. Additionally, anionic solutions decreased adsorption because of competition with the anions in the adsorbing phosphate. Although affected by the presence of competing anions or a humic substance, Fe-Mn-Si oxide has better adsorption capacity than Fe-Mn oxide.

요약문 : 국내 하수처리장 인 방류기준이 강화되어 다양한 방법의 인 제거기술이 적용되고 있다. 흡착은 비교적 간단하면서 효과적으로 인을 제거할 수 있다. 본 연구에서는 흡착제인 Fe-Mn-Si oxide와 Fe-Mn oxide을 개발하여, 인 제거효율을 검토하였으며 이 흡착제에 대하여 Kinetic과 Isotherm모형을 비교하였다. 두 흡착제의 최대흡착량은 각각 47.8, 35.5 mg-PO₄³⁻/g이었고, 이들은 낮은 pH에서 효과적으로 흡착하였다. Freundlich isotherm 모델이 Langmuir 모델보다 Fe-Mn-Si oxide의 흡착에 더 적합했다. 이온성 용액은 인이 흡착되는 과정에서 음이온들과 경쟁관계로 흡착능이 감소되었다. 비록 음이온과 humic물질들로부터 흡착에 영향을 받지만 Fe-Mn-Si oxide는 Fe-Mn oxide보다 흡착능이 크게 나타났다.

Key words : adsorbent, Fe-Mn-Si, Freundlich, Langmuir, phosphate, physicochemical

주제어 : 흡착제, Fe-Mn-Si, Freundlich, Langmuir, 인, 물리화학

1. Introduction

Waste containing phosphate is produced in large quantities in the industrial production of materials such as fertilizers, deter-

gents, food and drinks and the smelting and refining of various metals. These phosphate byproducts are discharged into municipal and industrial water effluent streams, affecting surface-water quality via the well-known process of eutrophication (Galarneau and Gehr, 1997; Karageorgiou *et al.*, 2007).

• Received 26 September 2013, revised 14 October 2013, accepted 15 October 2013.
* Corresponding author: Tel : 041-550-3516 E-mail : dockko@dankook.ac.kr

To handle excess phosphate discharge, the removal of phosphate employing various technologies has been investigated using physical (Clark *et al.*, 1997; Omoike and Vanloon, 1999), chemical (Ruixia *et al.*, 2002) and biological (Stensel, 1991) methods. However, chemical precipitation and biological removal have distinct disadvantages. Adsorption methods, on the other hand, have long been preferred owing to their low cost, effective treatment of dilute solutions of phosphates and excellent adsorption capacity (Zhang *et al.*, 2009). Beginning in 2012, the maximum discharge limit of total phosphorous in Korea was tightened from 2.0 to 0.2 mg/L. Inefficient conventional treatments cannot achieve this new requirement. However, the adoption of physicochemical processes using adsorbents will be advocated by environmental engineers and water facility operators because of their low cost and high efficiency. Different types of low-cost, high-capacity materials have long been used to remove phosphate, such as granulated coal ash (Asaoka and Yamamoto, 2010), red mud (Liu *et al.*, 2007; Zhao *et al.*, 2009; Yue *et al.*, 2010) and lanthanum-doped vesuvianite (Li *et al.*, 2009). Researchers have investigated ferric manganese oxide as an adsorbent for phosphate and arsenic removal (Zhang *et al.*, 2007, 2009). Current interest in phosphate adsorbents stems from phosphorus and arsenic both belonging to periodic group V and thus possessing similar chemical properties (Gao and Mucci, 2003). As a result, a recent publication studying silica-containing iron oxide as an adsorbent for arsenic removal

suggests that the addition of silica to iron (Fe) oxide could enhance its phosphate adsorption capacity (Zeng, 2003).

This research investigates the phosphate adsorption capacities of Fe–Mn–Si and Fe–Mn oxides and compares their performance via data analysis. The purpose of this study is to report the improvement in adsorption performance when inorganic silicon is added to ferric manganese oxide adsorbent.

2. Methods

2.1 Materials

Adsorbents were synthesized using a precipitation method and the chemicals potassium permanganate (KMnO_4), ferrous sulfate heptahydrate ($\text{FeSO}_4 \cdot 7\text{H}_2\text{O}$) and ferric chloride (FeCl_3) with and without added silicon dioxide anhydrous (SiO_2). Phosphate solutions were prepared by dissolving potassium dihydrogen orthophosphate (KH_2PO_4), manufactured by J. T. Baker (USA); the pH was adjusted using solutions of NaOH and/or HNO_3 (Duksan Chemical).

2.2 Adsorbent preparation

In the laboratory, Si was added to ferric manganese oxide employing a coprecipitation process. Ferric chloride (FeCl_3 , 7.31 g) was dissolved in 200 mL of distilled water. Ferrous sulfate heptahydrate ($\text{FeSO}_4 \cdot 7\text{H}_2\text{O}$, 12.51 g) and anhydrous silicon dioxide (SiO_2 , 18 g) were then added to this solution. Potassium permanganate (KMnO_4 , 2.37 g) solution was prepared by dissolving KMnO_4 in 200 mL of distilled

water. The iron and silicon were added to the potassium permanganate solution during vigorous stirring and the pH was adjusted to approximately 4–5 with the addition of 1 M NaOH solution. The solution was then stirred continuously for 1 hour. The precipitate formed at room temperature over the next 4 hours; finally, the precipitate was separated from the liquid portion. The sedimentation-containing liquor was then dried at 90 °C for 12 hours. The dried adsorbent, having a dark-brown color, was powdered and stored in a desiccator for later use. Fe–Mn–Si oxide was thus obtained. When anhydrous silicon dioxide was not added in the process, Fe–Mn binary oxide was produced.

2.3 Solution preparation

Synthetic water was prepared by adding $\text{Na}_2\text{HPO}_4 \cdot 7\text{H}_2\text{O}$ to distilled water. To investigate the effect of anions such as Cl^- and SO_4^{2-} on the process of adsorption, 1 mM sodium chloride (NaCl) solution and 10 mM sodium sulfate (Na_2SO_4) solution were prepared.

2.4 Apparatus

Ion chromatography (Metrohm, 881 Compact IC) was employed to determine the phosphate concentration throughout the experiment. A zeta potential analyzer (Zeta-Meter, USA) was used to measure the electrokinetic characteristics of the adsorbents. The surface morphology and adsorption capacity were measured employing scanning electron microscopy (SEM) and a batch experiment.

2.5 Experimental procedure

2.5.1 Zeta potential and SEM analysis

The zeta potentials of Fe–Mn–Si and Fe–Mn adsorbents were analyzed with a zeta potential analyzer under different pH conditions. The background electrolyte of the solutions was 100 mg/L NaCl to maintain constant ionic strength. SEM was employed to analyze the Fe–Mn–Si oxide before and after reaction with phosphate solution having a concentration of 35 mg PO_4^{3-} /L for a contact time of 10 min.

2.5.2 Adsorption kinetics and isotherms

Adsorption kinetics experiments were carried out using phosphate solutions with concentrations of 35 mg PO_4^{3-} /L at room temperature ($25 \text{ }^\circ\text{C} \pm 1 \text{ }^\circ\text{C}$). Quantities of 0.2 g of each adsorbent were added to a 1 L beaker and a 10 mL sample was taken at 5, 10, 20 and 30 min and 1, 2, 4, 8 and 24 hrs. All solutions were mixed with a magnetic stirrer at an agitation speed of 140 rpm throughout the reaction. The pH was adjusted to 4.5 ± 1 . The samples were then passed through a 0.45 μm filter before analyzing the phosphate residual. In the isotherm experiments, 5, 10, 20, 30, 40, 50, 60, 70, 80 and 90 mg quantities of each adsorbent were placed with phosphate solutions of 35 mg- PO_4^{3-} /L in 50 mL vials. The vials were shaken for 24 hrs at a speed of 140 rpm.

2.5.3 Effect of pH, coexisting anions and desorption

The effect of coexisting anions, namely

Cl⁻ and SO₄²⁻, was investigated at different pH values by adding 1 mM NaCl and 10 mM Na₂SO₄, respectively. The contact time was 5 min for each 2 g/L dose of adsorbent. In the study of desorption, the adsorbents were saturated with 35 mg-PO₄³⁻/L solution for 24 hrs. The amount of adsorbed phosphate was calculated by measuring the supernatant of the solution. The saturated adsorbents were filled with 0.001, 0.01 and 0.1 M NaOH, 10 mM NaCl, 10 mM Na₂SO₄ and 4 mg/L humic acid solutions. The solutions were stirred for 30 min at a speed of 140 rpm. Finally, the desorbed amount of phosphate was calculated by subtracting the residual phosphate from the initially adsorbed amount of phosphate.

2.6 Analytical methods

2.6.1 Langmuir and Freundlich isotherm models

By applying the experimental data to Langmuir and Freundlich models, it is possible to determine the adsorption capacity of Fe-Mn-Si and Fe-Mn oxides in different concentrations of phosphate solution (Gao and Mucci, 2003; Zeng, 2003; Elzinga and Sparks, 2007). Model equations are given below.

$$\text{Freundlich model: } q_e = K_F C_e^{1/n} \quad (1)$$

Here, q_e is the amount of phosphate adsorbed per gram of adsorbent (mg/g); C_e is the total phosphate concentration of the solution (mg-PO₄³⁻/L); the Freundlich constant K_F reflects the adsorption capacity of the adsorbent; and the experimental constant n represents the adsorption capacity of the adsorbent. n is a heteroge-

neity factor that has a lower value for a more heterogeneous surface.

$$\text{Langmuir model: } q_e = q_m K_L C_e / (1 + K_L C_e) \quad (2)$$

Here, the factors q_e and C_e have been previously noted; K_L is the equilibrium adsorption constant describing the affinity of binding sites (L/mg); and q_m is the maximum amount of the phosphate per unit weight of adsorbent.

2.6.2 Pseudo second-order model

The adsorption rate can be calculated from the duration of the adsorption process and analyzed using the pseudo second-order models of adsorption kinetics (Ho, 2006; Lindegren and Persson, 2010).

Pseudo second-order model :

$$q_t = k_2 q_e^2 t / (1 + k_2 q_e t) \quad (3)$$

Here, q_t is the amount of adsorbate sorbed on the sorbent surface at time t (mg/g); k_1 is the first-order rate constant of sorption (g/mg/min); k_2 is the second-order rate constant of sorption (g/mg/min); q_e is the amount of adsorbate removed from aqueous solution at equilibrium (mg/g); and t is the reaction time (min).

3. Results and discussion

3.1 Zeta potential

The zeta potentials of Fe-Mn-Si and Fe-Mn oxides under different pH conditions decreased with increasing pH. As shown in Fig. 1, the zero point of charges (pH_{zpc}) of Fe-Mn-Si and Fe-Mn were about 3.3±0.2 and 6.0±0.2, respectively. The negative charge of Fe-Mn-Si adsorbent

is due to the Si-OH structure (Manning and Goldberg, 1997). Specific adsorption of phosphate as an anion makes the surface of oxides more negatively charged, which shifts the isoelectric point of the adsorbent to a lower pH value (Hsia *et al.*, 1994).

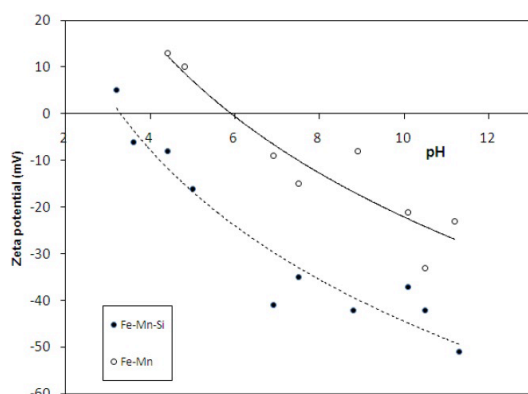


Fig. 1. Zeta potentials of Fe-Mn-Si and Fe-Mn oxides.

3.2 Adsorption kinetics

The kinetics of adsorption using equations (1), (2), (3) were determined from the contact time of the adsorption process for different initial phosphate concentrations. Results of the pseudo second-order model fit are shown in Fig. 2 together with the experiment kinetics results.

The initial phosphate concentrations were 35 mg/L and the initial pH value of the solution was 4.5. In the first 2 hrs, 70 % of the equilibrium adsorption capacity was achieved in the case of Fe-Mn-Si oxide. The adsorption capacity of Fe-Mn-

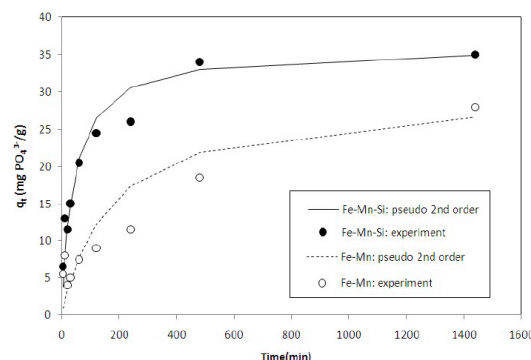


Fig. 2. Pseudo second-order model fits of experiment kinetics data for Fe-Mn-Si and Fe-Mn oxide adsorbents.

Si oxide was higher than that of Fe-Mn oxide. To calculate the rate of adsorption analytically, pseudo second-order models were employed using experimental data of phosphate adsorption (Ho, 2006). The pseudo second-order model fit the experimental data well with a high correlation coefficient of 0.935–0.998. All parameter values used in developing the pseudo second-order models are listed in Table 1.

3.3 Adsorption isotherm

The adsorption isotherms considering the effects of the equilibrium concentration on the adsorption capacity are shown in Fig. 3. Data were analyzed using Freundlich and Langmuir isotherm models. The results and parameters of these models are given in Table 1. The Freundlich model fits the experimental data of the Fe-Mn-Si and Fe-Mn oxides well with relatively high

Table 1. Parameters of pseudo second-order, Freundlich and Langmuir models for the adsorption of phosphate

Oxide type	Pseudo second-order model			Freundlich model			Langmuir model		
	q_e (mg/g)	k_2 (g/mg/min)	R^2	$1/n$	K_f (L/mg)	R^2	q_m (mg/g)	K_L (L/mg)	R^2
Fe-Mn-Si	35.9	0.000652	0.998	0.266	21.860	0.949	47.849	0.791	0.929
Fe-Mn	29.7	0.000196	0.935	0.246	17.855	0.977	35.460	0.949	0.825

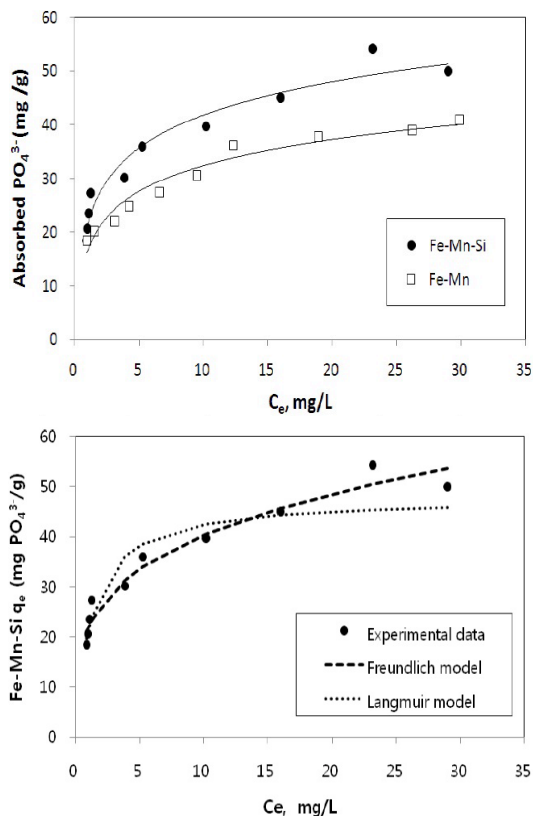


Fig. 3. Isotherms of phosphate adsorption by Fe-Mn-Si and Fe-Mn oxides.

correlation coefficients (R^2) of 0.949 and 0.977, respectively. The maximum capacity of this adsorbent was $47.8 \text{ mg-PO}_4^{3-}/\text{L}$, which was derived from the Langmuir model. The Freundlich model can be well applied to solids with heterogeneous surface properties. On the other hand, the fit of Fe-Mn adsorption had a poor correlation value ($R^2 = 0.825$). Previous research has shown that the maximum adsorption capacity of Fe-Mn oxide is $33.2 \text{ mg-PO}_4^{3-}/\text{L}$ at a pH of 5.6 ± 1 (Zhang *et al.*, 2009). Consequently, Fe-Mn-Si has greater adsorption capacity than Fe-Mn oxide.

3.4 Effects of pH and coexisting anions on adsorption

The effects of pH and coexisting anions on the two adsorbents are shown in Fig. 4. It is clear that when the solution pH increases, the phosphate adsorption by both adsorbents decreases. Similarly, both Fe-Mn-Si and Fe-Mn oxides have greater adsorption capacity at low pH than at high pH. The explanation is that at high pH, the adsorbent surface becomes more negatively charged, increasing the repulsion between the phosphate cation and the adsorbent surface (Lindegren and Persson, 2010). Moreover, the ionic solution concentration also affects adsorption.

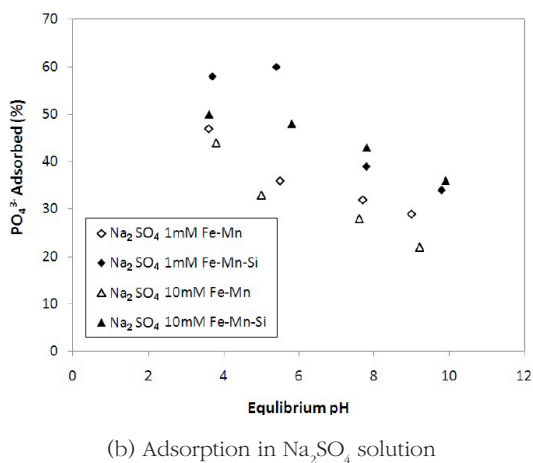
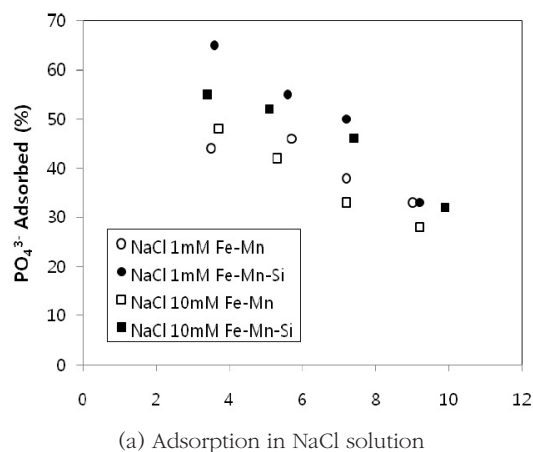


Fig. 4. Effects of pH and coexisting anions on the adsorption of Fe-Mn-Si and Fe-Mn oxides.

Adsorption decreased slightly at a high concentration of coexisting anions, but it increased at low concentrations. The coexisting anions exerted less influence on the adsorption on Fe–Mn–Si oxide, allowing greater adsorption than was observed for Fe–Mn oxide. It is clear that a change in ionic strength from 1 to 10 mM played a role in decreasing the adsorption of phosphate. However, the valence of anions had little effect on the adsorption. This agrees with the finding that the phosphate ions strongly adsorbed at specific sites are rarely exchangeable even in a solution with a large excess of coexisting ions (Zhang *et al.*, 2009). In inner-sphere complexes of adsorbent, the surface hydroxyl groups act as σ -donor ligands, which increase the electron density of the coordinated metal ion (Stumm, 1992). The adsorption of these anions was suppressed with weakly adsorbing anions such as Cl^- and SO_4^{2-} , as these electrolytes also formed outer-sphere complexes through electrostatic forces. These anions that were adsorbed by the inner-sphere association either showed little sensitivity to ionic strength or responded to higher ionic strength with greater adsorption. The binding of a metal ion by surface ligands is strongly pH-dependent as shown in Fig. 4.

3.5 Desorption

Desorption was carried out using three different concentrations of alkaline solutions, two different anions and an organic substance. The percentage of desorbed phosphate is shown in Fig. 5. With the

addition of NaOH, alkaline solution concentrations of 0.001, 0.01 and 0.1 M were created. The Fe–Mn–Si oxide and Fe–Mn oxide were then added to these three alkaline solutions. It is clear that the amount of phosphate desorption increased with an increase in alkalinity. The amount of phosphate desorbed by the Fe–Mn–Si oxide and Fe–Mn oxide was found to increase from 42 % to 59 % and from 2 % to 86 % as the solution concentrations increased from 0.001 to 0.1 M, respectively. The effect of the alkaline solutions on the desorption process was relatively weak for Fe–Mn–Si oxide but strong for Fe–Mn oxide. Furthermore, when adding the adsorbents to phosphates in the presence of the mono/divalent anions and organic substance, the desorption of phosphate approached that achieved in alkaline solutions. These results show that the phosphate-loaded Fe–Mn oxide can be more easily desorbed than Fe–Mn–Si oxide in NaOH solution. This means that Fe–Mn oxide has the potential to be used as a regenerated adsorbent for phosphate removal.

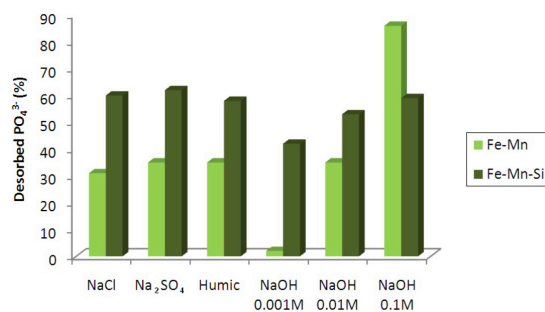


Fig. 5. Desorption performance after adsorption of phosphate by Fe–Mn–Si and Fe–Mn oxide adsorbents depending on the concentration of alkaline solution, anions and addition of an organic substance.

The morphology of Fe–Mn–Si oxide obtained by SEM is shown in Fig. 6(a, b). The figure illustrates the difference in morphology between these two adsorbents before and after phosphate adsorption. The image of the Fe–Mn–Si adsorbent shows that the adsorbent consisted of many small particles having porous structures and rough surfaces. After phosphate adsorption, the morphology was not significantly different.

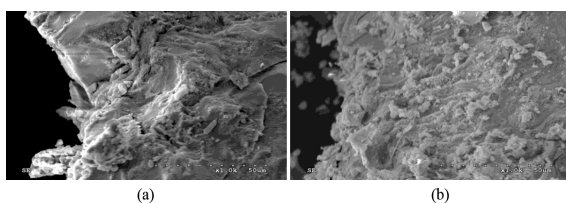


Fig. 6. SEM morphology of Fe-Mn-Si oxide (a) before and (b) after phosphate adsorption.

4. Conclusion

In a comparative study of two new adsorbents, the addition of inorganic silicon to Fe–Mn oxide was shown to improve adsorption performance. The adsorption of both adsorbents was affected directly by pH: the adsorption capacity increased at low pH but decreased at high pH. Investigation revealed that a change in ionic strength from 1 to 10 mM decreased the adsorption of phosphate. However, the valence of anions had little effect on the adsorption. The isotherm of the Freundlich model predicted the adsorption of Fe–Mn–Si better than the Langmuir model. A pseudo second-order model is suitable for analyzing the adsorption kinetics. Anionic solutions and a humic substance decreased adsorption through competition between

these anions and the phosphate anions in the adsorption of phosphate. Although affected by the presence of competing anions or a humic substance, Fe–Mn–Si oxide has better adsorption capacity than Fe–Mn oxide.

Acknowledgements

This research was supported through the National Research Foundation of Korea (NRF) funded by the Ministry of Education, Science and Technology (013–2011–1–D00071) and partly funded by a grant from the Eco–Innovation (Gbest) Project.

References

- Asaoka S. and Yamamoto T. (2010). Characteristic of phosphorus adsorption onto granulated coal ash in seawater. *Marine Pollution Bulletin*, **60**(8), 1188–1192.
- Clark T., Stephenson T. and Pearse P. A. (1997). Phosphorus removal by chemical precipitation in biological aerated filter. *Water Research*, **31**, 2557–2563.
- Elzinga E. J. and Sparks D. L. (2007). Phosphorus adsorption onto hematite: an in situ ATR-FTIR investigation of effects of pH and loading level on the mode of phosphorus surface complexation. *Journal of Colloid and Interface Science*, **308**, 53–70.
- Galarneau E. and Gehr R. (1997). Phosphorus removal from wastewaters: experimental and theoretical support for alternative mechanisms. *Water Research*, **31**, 328–338.
- Gao Y. and Mucci A. (2003). Individual and competitive adsorption of phosphorus and arsenate on goethite in artificial seawater. *Chemical Geology*, **199**, 91–109.
- Ho Y. S. (2006). Review of second-order models for adsorption system. *Journal of Hazardous Materials*, **136**, 681–689.
- Karageorgiou K., Paschalis M. and Anastassakis G. N. (2007). Removal of phosphorus spe-

- cies from solution by adsorption onto calcite used as natural adsorbent. *Journal of Hazardous Materials*, **39**, 447–452.
- Li H., Ru J., Yin W., Liu X., Wang J. and Zhang W. (2009). Removal of phosphorus from polluted water by lanthanum doped vesuvianite. *Journal of Hazardous Materials*, **168**, 326–330.
- Lindegren M. and Persson P. (2010). Competitive adsorption involving phosphorus and benzenecarboxylic acids on goethite – effect of molecular structures. *Journal of Colloid and Interface Science*, **343**, 263–270.
- Liu C. J., Li Y. Z., Luan Z. K., Chen Z. Y., Zhang Z. G. and Jia Z. P. (2007). Adsorption removal of phosphorus from aqueous solution by active red mud. *Journal of Environmental Science*, **19**, 1166–1170.
- Omoike A. I. and Vanloon G. W. (1999). Removal of phosphorus and organic matter removal by alum during wastewater treatment. *Water Research*, **33**, 3617–3627.
- Ruixia L., Jinlong G. and Hongxiao T. J. (2002). Adsorption of fluoride, phosphate, and arsenate ions on a new type of ion exchange fiber. *Journal of Colloid and Interface Science*, **248**, 268–274.
- Yue Q., Zhao Y., Li Q., Li W., Gao B., Han S., Qi Y. and Yu H. (2010). Research on the characteristics of red mud granular adsorbents (RMGA) for phosphorus removal. *Journal of Hazardous Materials*, **176**, 741–748.
- Zeng L. (2003). A method for preparing silica-containing iron (III) oxide adsorbents for arsenic removal. *Water Research*, **37**, 4351–4358.
- Zhang G., Qu J., Liu H., Liu R. and Wu R. (2007). Preparation and evaluation of a novel Fe/Mn binary oxide adsorbent for effective arsenite removal. *Water Research*, **41**, 1921–1928.
- Zhang G., Liu H., Liu R. and Qu J. (2009). Removal of phosphorus from water by a Fe/Mn binary oxide adsorbent. *Journal of Colloid and Interface Science*, **335**, 168–174.
- Zhao Y., Wang J., Luan Z., Peng X., Liang Z. and Shi L. (2009). Removal of phosphorus from aqueous solution by red mud using factorial design. *Journal of Hazardous Materials*, **165**, 1193–1199.